

Ultrafast acoustical gating of the photocurrent in a p - i - n tunneling diode incorporating a quantum well

D. Moss, A. V. Akimov, O. Makarovskiy, R. P. Campion, C. T. Foxon, L. Eaves, and A. J. Kent*
School of Physics and Astronomy, University of Nottingham, University Park, Nottingham NG7 2RD, United Kingdom

B. A. Glavin

Institute of Semiconductor Physics, National Academy of Sciences, Kiev 03028, Ukraine

(Received 4 August 2009; published 23 September 2009)

Ultrafast acoustic wave packets are used to control the photocurrent excited by a femtosecond optical pulse in a reverse biased $\text{Al}_x\text{Ga}_{1-x}\text{As}$ p - i - n tunneling diode containing a GaAs quantum well in its intrinsic region. The change in photocurrent arises from the strain-induced shift of the quantum well excitonic resonance due to deformation potential electron-phonon coupling. This method of controlling electron transport on an ultrafast time scale could form the basis of a new class of terahertz electronic devices.

DOI: [10.1103/PhysRevB.80.113306](https://doi.org/10.1103/PhysRevB.80.113306)

PACS number(s): 72.80.Ey, 72.50.+b, 85.30.Mn

The control of electronic device properties on ever faster time scales has long been a challenge for researchers and technologists. Conventional devices, which operate with voltages and currents applied to metalized contacts, are currently limited to frequencies of several GHz. For faster manipulations, terahertz (THz) and ultrafast optical techniques may be used. Another possible approach is based on the use of high-frequency acoustic waves. Acoustic techniques at GHz frequencies have proved to be a powerful tool for controlling the optical and electronic properties of semiconductor nanostructure devices.^{1,2} The use of picosecond acoustics could increase the frequency into the THz range. Methods developed during the last two decades provide for the generation and detection of: picosecond strain pulses and wave packets;^{3,4} acoustic solitons;⁵ THz and harmonic elastic oscillations in superlattices^{6,7} and phonon microcavities.⁸ The effects of picosecond strain pulses on the optical reflectivity and photoluminescence spectra in semiconductor nanostructures have demonstrated the feasibility of ultrafast control of the optical properties by means of picosecond acoustic techniques.⁹ However, the control, on a picosecond time scale, of the electrical transport properties of a device using acoustic waves is still to be realized.

Here we describe picosecond photocurrent experiments in which strain and optical pulses act simultaneously upon the quantum well (QW) embedded in the intrinsic layer of a p - i - n tunneling diode. The strong sensitivity of the electron-hole (i.e., exciton) excitation energy, E_0 , in the QW to the applied strain ε , known as the piezospectroscopic effect,¹⁰ is exploited. By using the strain pulse $\varepsilon(t)$ to modulate E_0 , we are able to tune or detune the exciton resonance with the energy, $\hbar\omega$, of the incident photons from a laser probe beam. The optical absorption, and hence the number of photoexcited carriers in the QW, depends on $(E_0 - \hbar\omega)$ and thus follows $\varepsilon(t)$. In the presence of an applied electric field, F , a large fraction of the photoexcited carriers tunnels through the barriers of the QW and thereby contributes to the photocurrent (see inset in Fig. 1). Thus, the photocurrent, which is proportional to the number of carriers excited by the light pulse at time t , is related directly to $\varepsilon(t)$ in the QW. Essentially the strain pulse plays the role of an ultrafast gate con-

trolling the photocurrent in p - i - n diode in which the QW is the absorbing media.

The p - i - n device used in the experiments was grown by molecular beam epitaxy on a semi-insulating GaAs substrate of a thickness $l=375 \mu\text{m}$. The active structure consists of a single 7.5 nm-thick undoped GaAs QW confined between

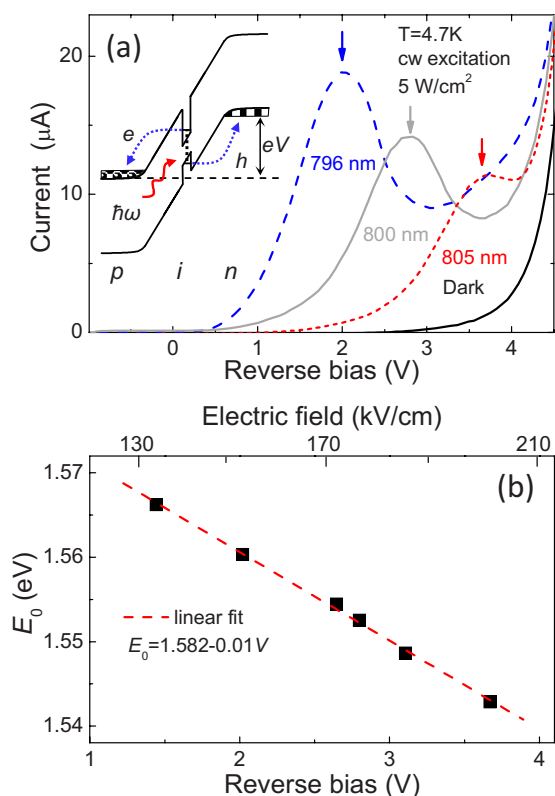


FIG. 1. (Color online) (a) I - V curves measured in the dark and under illumination for different wavelengths of CW optical excitation. The inset shows the optical and tunneling transitions in the QW in the applied electric field. (b) Bias dependence of the exciton resonance energy E_0 in the QW obtained from the position of peaks in the I - V curves for various excitation wavelengths. The upper horizontal scale shows the electric field in the QW calculated from the experimental values of E_0 .

two 100 nm-wide undoped $\text{Al}_{0.3}\text{Ga}_{0.7}\text{As}$ layers. The n and p contacts were, respectively, Si-doped and C-doped (both 10^{18} cm^{-3}) 200 nm-wide layers of $\text{Al}_{0.3}\text{Ga}_{0.7}\text{As}$, respectively. The structure was processed into 400 μm diameter mesas with ring-shaped electrical contacts to allow optical access. A schematic band diagram of the p - i - n RTD under reverse bias is shown in the inset of Fig. 1.

The experiments were performed in an optical cryostat at $T=4.7 \text{ K}$. To characterize the device and obtain values of E_0 as a function of reverse bias, V , the current-voltage (I - V) characteristics, shown in Fig. 1(a), were measured in the dark and under CW photoexcitation at different wavelengths. The peaks in the photocurrent, indicated by the vertical arrows in Fig. 1(a), correspond to the condition when the photon energy $\hbar\omega \approx E_0$.¹¹ The applied reverse bias, V , reduces the value of E_0 in the QW due to the quantum-confined Stark effect¹² and, hence, the bias value of the peak in the I - V curve increases with the increase in the excitation wavelength. The measured dependence of E_0 on V obtained from the I - V curves is shown in Fig. 1(b).

In the ultrafast experiments, the picosecond strain pulses were generated in a 100 nm thick Al-film deposited on the polished side of the GaAs substrate opposite to the p - i - n structure. The film was excited by ~ 50 femtosecond optical pump pulses with a wavelength of 800 nm and repetition rate 5 kHz. The laser beam was focused to a spot with a diameter 150 μm on the surface of the Al film exactly opposite to the optical mesa of the p - i - n structure. Due to the thermoelastic effect, a 10 ps duration bipolar strain pulse $\varepsilon(t, z)$, where z is the coordinate perpendicular to the interface of the substrate with the metal film, was generated in the film. The strain pulse was injected from the Al film to the GaAs substrate and reached the p - i - n structure after traversing the GaAs substrate in a time $t_0 = l/s_L = 78 \text{ ns}$ where $s_L = 4.8 \times 10^3 \text{ m/s}$ is the longitudinal (LA) sound velocity in GaAs.

The experimental setup for detecting the effect of the strain pulse in the p - i - n structure is shown in Fig. 2(a). The p - i - n diode was excited by a femtosecond optical probe beam split from the same laser that was used to excite the Al film. The beam was passed through a 23 m long delay line which provided a time delay $\sim t_0$. The spectrum of the probe pulse was centered at $\hbar\omega = 1.55 \text{ eV}$ and had width of 60 meV. The beam was focused to a spot of 150 μm at the center of the optical mesa with an energy density $< 10 \mu\text{J}/\text{cm}^2$. The probe pulse excited a microsecond-long photocurrent pulse in the device as shown in the frame in Fig. 2(a). The signal was amplified, and the time-integrated photocurrent signal P was measured as a function of time delay t between the optical pump and probe pulses. In order to pick out the strain-induced signal $\Delta P(t) = P(t) - P_0$ (P_0 is the signal without a strain pulse) the pump pulse was chopped with a frequency 500 Hz and a lock-in amplifier was used for the detection of $\Delta P(t)$.

Figure 2(b) shows the temporal evolution of the strain-induced photocurrent changes $\Delta P(t)/P_0$ measured for two values of the reverse bias, V , and for two pump energy densities, W . Ultrafast temporal changes of $\Delta P(t)$, observed on a constant positive background, start with the decrease in photocurrent. For the chosen values of $E_0 > \hbar\omega$, such behavior corresponds to the increase in E_0 . In a GaAs QW this hap-

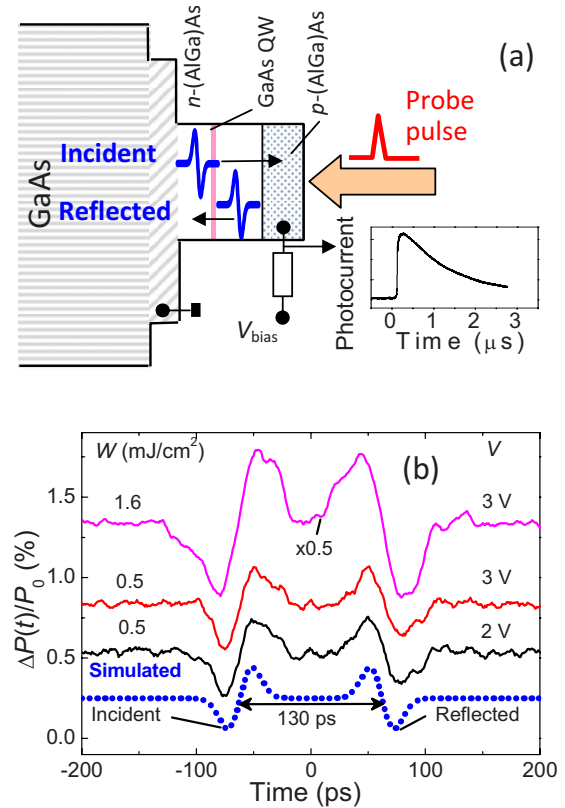


FIG. 2. (Color online) (a) The schematic diagram of ultrafast probing of the photocurrent changes in the p - i - n structure, showing the bipolar strain pulses arriving at the QW due to the initial strain pulse and the pulse reflected from the top surface of the device. (b) The temporal traces (solid lines) of the relative photocurrent changes measured for two bias voltages V and pump densities W . The dotted line shows the simulated temporal trace when the incident and reflected bipolar strain pulses pass through the QW.

pens if the leading part of the strain pulse $\varepsilon(t)$ is compressive, i.e., $\varepsilon < 0$, as is well known to be the case in picosecond acoustic experiments with optical excitation of a metal film.^{4,5} Next, the tensile part of $\varepsilon(t)$ reaches the QW and $\Delta P(t)$ increases. This bipolar behavior is repeated in reverse order after a delay of 130 ps due to the passage of a reflected pulse, as explained below.

All traces in Fig. 2(b) fit quantitatively the simulated temporal curve, obtained when only the effect of the strain pulse on the number of photoexcited carriers in the QW is considered and shown by the dotted line in Fig. 2(b). The spatial length $\sim 200 \text{ nm}$ of the strain pulse is much wider than the QW and thus, at each point of time t the strain $\varepsilon(t)$ in the QW may be considered constant. The two bipolar pulses in $\Delta P(t)$ correspond to the arrival of the QW of incident and reflected strain pulses propagating from the GaAs substrate toward the top surface of the p - i - n structure and back from the surface toward the GaAs substrate, respectively [see Fig. 2(a)]. The 130 ps difference in the arrival times of the incident and reflected pulses to the QW is the propagation time for longitudinal polarized sound over the distance of 620 nm from the QW to the surface and back. The incident and reflected pulses have opposite phases due to the phase change at reflection. The value $t=0$ in Fig. 2(b) is chosen as a time

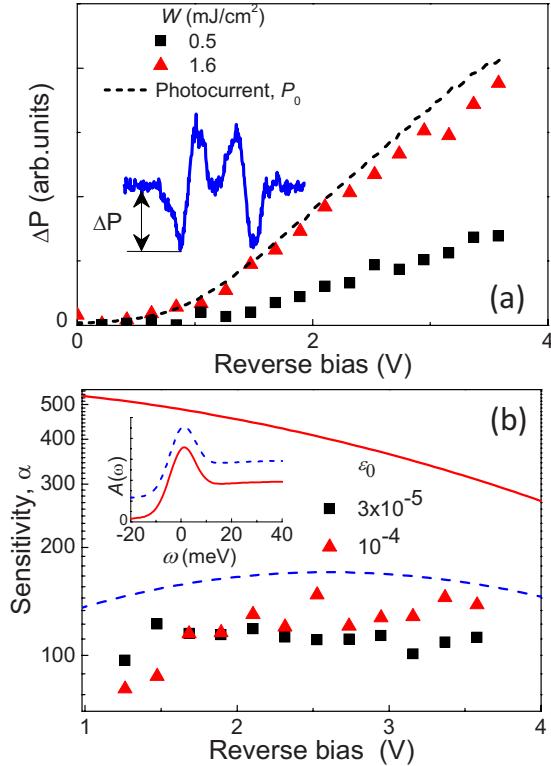


FIG. 3. (Color online) (a) The symbols show the dependencies of the amplitude ΔP of the ultrafast photocurrent changes on the reverse bias V for two pump energy densities W . The dashed curve is the bias dependence of the photocurrent in the absence of the strain pulses. The inset shows the method of obtaining ΔP from the temporal signal $\Delta P(t)$. (b) The measured (symbols) for two strain pulse amplitudes ε_0 and calculated (lines) dependences of the photocurrent sensitivity α to the strain. The solid and dashed lines correspond to the absorption spectra $A(\omega)$ shown in the inset by the solid and dashed lines respectively. The $\omega=0$ in the inset corresponds to the energy of the exciton resonance.

when the center of $\varepsilon(t)$ reaches the surface of the sample.

It is seen in Fig. 2(b), for fixed W , the temporal shape of $\Delta P(t)$ is almost independent of V . Figure 3(a) shows the dependence on bias of the signal amplitude ΔP_0 due to the incident pulse [see inset to Fig. 3(a)]. This dependence is similar to that of the photocurrent P_0 on V , measured without strain pulses and shown in Fig. 3(a) by the dashed line. Correspondingly, the strain-induced relative changes $\Delta P_0/P_0$ is almost independent of V . Increasing W results in the increase in ΔP_0 and temporal broadening of the detected signals, which can be seen from the comparison of traces in Fig. 2(b) for two values of W . The dependence of ΔP_0 on W is linear up to $W=1.5$ mJ/cm², while for higher W a sublinear behavior with the tendency toward saturation is observed.

The key result of the experiments is the observation of the pump-probe signal, which follows the temporal evolution of the picosecond strain pulse $\varepsilon(t)$ in the QW. Unambiguous evidence for this is that the incident and reflected pulses are separated by $\Delta t=130$ ps, which is exactly the propagation time of the pulse from the QW to the surface and back to the QW again. Therefore, when probing by the laser pulse with $\hbar\omega \sim E_0$, any ultrafast strain-induced effects produced when

the strain pulse passes through other parts of the device make no significant contribution to the photocurrent.

For the quantitative analysis presented below it is necessary to know the value of the electric field F in the QW and its dependence on V . This was obtained from calculations of the electron and hole eigenstates in the QW as a function of F and, further, comparing this with the measured dependence of E_0 on V presented in Fig. 1(b). The measured dependence of F on V is almost linear and can be found from the comparison of the upper and lower scales in Fig. 1(b). Theoretical analysis based on the band diagram, schematically shown in the inset of Fig. 1(a), gives the effective thickness of the insulator layer in the $p-i-n$ structure: $d_i=(eV+E_g)/F$ (where E_g is the band gap in the doped AlGaAs contacts). At liquid helium temperatures, the value of d_i increases noticeably with V and is 20–40% larger than the nominal grown thickness (207.5 nm) due to the depletion regions in the (AlGa)As contacts. The relatively low free-carrier density $\sim 10^{17}$ cm⁻³ in the p -contact at $T=4.7$ K, estimated from the dependence of F on V is confirmed by capacitance-voltage measurements, which show that the (AlGa)As contacts are partially frozen out at these low temperatures.

Using the dependence of F on V we estimate the changes in the photocurrent provided by the acoustical gating for various mechanisms of the electron-phonon interaction in the QW. The temporally integrated photocurrent generated by the carriers excited optically in the QW may be written as:

$$P = \frac{2eN\tau_{\text{rad}}}{\tau_t + \tau_{\text{rad}}}, \quad (1)$$

where N is the number of photoexcited electron-hole pairs in the QW; τ_t is the time of carrier tunneling from the QW; and τ_{rad} is carrier recombination time in the QW. Using the Wentzel-Kramers-Brillouin (WKB) approximation it is found that, for the relevant values of F [see Fig. 1(b)], $\tau_t \sim 1$ –100 ps, which is much less than $\tau_{\text{rad}} \sim 1$ ns. Therefore, from Eq. (1) it is found that the major fraction of photoexcited carriers contribute to the photocurrent.

The number of photoexcited electrons and holes is given by

$$N = \int d\omega \frac{I(\omega)}{\hbar\omega} A(\omega), \quad (2)$$

where $I(\omega)$ is the spectral density of the optical energy flux and $A(\omega)$ is the QW absorption efficiency. In ultrafast experiments, $I(\omega)$ can be approximated by a Gaussian, $I(\omega) \sim \exp[-\frac{(\omega-\omega_0)^2}{2\Delta\omega^2}]$, where the broadening parameter, $\Delta\omega \approx 25$ meV.

In analyzing the effect of strain on the photocurrent, it is at first assumed that the kinetic parameters τ_t and τ_{rad} are insensitive to strain. Then the strain induced changes of P are governed only by the modification of $A(\omega)$. The spectral shape of $A(\omega)$ can be modeled by the curves shown in the inset of Fig. 3(b). The peak and the high-energy wing correspond to the exciton and free electron-hole transitions, respectively.¹¹ The strain ε modifies $A(\omega)$ by changing the band gap in the QW due to the deformation potential, i.e., $A(\omega)=A_0(\omega)-\frac{dA}{d\omega}E_1\varepsilon/\hbar$, where $A_0(\omega)$ is the absorption spec-

trum at $\varepsilon=0$ and E_1 is the deformation potential (for GaAs $E_1 \approx -10$ eV). The strain-induced relative changes in the photocurrent then can be written as

$$\frac{\Delta P}{P_0} = - \frac{E_1 \varepsilon \int d\omega I(\omega) \frac{dA}{d\omega}}{\hbar \int d\omega I(\omega) A(\omega)}. \quad (3)$$

In addition to the deformation potential, there are other mechanisms, which can cause strain-induced changes in $A(\omega)$.^{13–15} Numerical estimates for our device indicate that all these effects are small, typically less than 10% of the contribution from the deformation potential.

The lines in Fig. 3(b) shows the bias dependences of the sensitivity $\alpha = \Delta P / \varepsilon P_0$ of the detected signal ΔP to ε calculated using Eq. (3). The symbols in Fig. 3(b) correspond to the experimental data for two values of strain amplitude, ε_0 , estimated for the corresponding W using the standard methods of ultrafast acoustics with the duration of the strain pulse taken as a fitting parameter.^{3,4,9,16} The curve (solid line) in Fig. 3(b) is deduced using the $A(\omega)$ lineshape shown by the solid curve in the inset of Fig. 3(b). In this case, the calculated values of α decrease significantly with increasing V , whereas the experimental data does not show strong dependence on V . Better agreement with experiment [dashed line in Fig. 3(b)] can be obtained by assuming that $A(\omega)$ has an additional energy independent background (see the dashed curve in the inset). The background does not contribute to ΔP , but increases the photocurrent P_0 , which results in the decrease in sensitivity. The inclusion of such a background is justified by the likely presence of other channels for the generation of carriers in addition to photoexcitation in the QW (e.g., the Franz-Keldysh effect or photoexcitation of localized carriers in the AlGaAs layers and elevated temperature in the pulsed experiments).¹¹

The analysis, based on Eq. (3), assumed that the kinetic parameters τ_t and τ_{rad} are strain-independent. This assumption is justified by the experimental result which shows weak dependence of the temporal shape $\Delta P(t)$ on V [compare two traces for $W=0.5$ mJ/cm² in Fig. 2(b)]. Indeed, any strain-induced changes of τ_t or τ_{rad} should be detected in the time interval that the carriers are present in the QW after the probe pulse. In this case, $\Delta P(t)$ is the result of the time convolution of the strain pulse $\varepsilon(t)$ and the temporal decay of the photoexcited carrier densities in the QW. The estimated values of $\tau_t \sim 1-100$ ps vary with V over orders of magnitude. Therefore, if τ_t and τ_{rad} were strain-dependant, the temporal shape of $\Delta P(t)$ would be strongly dependent on V , but this is not observed in the experiments.

The temporal broadening of $\Delta P(t)$ with increasing W , which can be seen in Fig. 2(b), and also the saturation of ΔP_0 at high W are possibly due to the nonlinear propagation properties of the strain wave packet in the GaAs substrate.^{5,17,18}

We have shown that a picosecond strain pulse can be used to gate, on a picosecond time scale, the photocurrent in a $p-i-n$ diode containing a QW in its intrinsic region. The effects are linked to the QW while all other regions of the device, such as the barriers and contacts, are not affected by the strain on this time scale. Regardless of the fact that the external circuit is limited to GHz speeds, these experiments demonstrate that ultrafast control of the internal electron processes using strain pulses is possible. This could lead to the development of techniques for clocking devices with THz acoustic waves. This method is not limited to a QW $p-i-n$ diode, and could be extended to quantum dot nanostructures and various tunneling devices with the strain-sensitive electronic resonances.

We acknowledge support from the UK Engineering and Physical Sciences Research Council and the Royal Society.

*anthony.kent@nottingham.ac.uk

¹M. M. de Lima, Jr., M. van der Poel, P. V. Santos, and J. M. Hvam, Phys. Rev. Lett. **97**, 045501 (2006).

²M. R. Astley, M. Kataoka, C. J. B. Ford, C. H. W. Barnes, D. Anderson, G. A. C. Jones, I. Farrer, D. A. Ritchie, and M. Pepper, Phys. Rev. Lett. **99**, 156802 (2007).

³C. Thomsen, H. T. Grahn, H. J. Maris, and J. Tauc, Phys. Rev. B **34**, 4129 (1986).

⁴O. B. Wright, Phys. Rev. B **49**, 9985 (1994).

⁵H.-Y. Hao and H. J. Maris, Phys. Rev. B **64**, 064302 (2001).

⁶A. Bartels, T. Dekorsy, H. Kurz, and K. Kohler, Phys. Rev. Lett. **82**, 1044 (1999).

⁷C.-K. Sun, J.-C. Liang, and X.-Y. Yu, Phys. Rev. Lett. **84**, 179 (2000).

⁸A. Huynh, B. Perrin, N. D. Lanzillotti-Kimura, B. Jusserand, A. Fainstein, and A. Lemaitre, Phys. Rev. B **78**, 233302 (2008).

⁹A. V. Akimov, A. V. Scherbakov, D. R. Yakovlev, C. T. Foxon, and M. Bayer, Phys. Rev. Lett. **97**, 037401 (2006).

¹⁰E. F. Gross and A. A. Kaplyanskii, Sov. Phys. Solid State **2**, 1518 (1961).

¹¹S. Schmitt-Rink, D. S. Chemla, and D. A. B. Miller, Adv. Phys. **38**, 89 (1989).

¹²D. A. B. Miller, D. S. Chemla, T. C. Damen, A. C. Gossard, W. Wiegmann, T. H. Wood, and C. A. Burrus, Phys. Rev. B **32**, 1043 (1985).

¹³B. A. Glavin, V. A. Kochelap, T. L. Linnik, and K. W. Kim, Phys. Rev. B **71**, 081305(R) (2005).

¹⁴F. T. Vasko and V. V. Mitin, Phys. Rev. B **52**, 1500 (1995).

¹⁵V. I. Pipa, V. V. Mitin, and M. Stroschio, Appl. Phys. Lett. **74**, 1585 (1999).

¹⁶The estimation of ε_0 has an accuracy not better than the order of magnitude because the dispersion, scattering, and elastic nonlinearity in GaAs are not taken into account.

¹⁷A. J. Kent and N. M. Stanton, J. Phys. Conf. Ser. **92**, 012004 (2007).

¹⁸E. Péronne and B. Perrin, Ultrasonics **44**, e1203 (2006).